










Cooperative Towing by Multi-Robot System That Maintains Welding Cable in Optimized Shape

Ryota Suzuki , Yoshito Okada , Yoshiki Yokota , Tatsuyoshi Saijo, Haruhiko Eto , Yuya Sakai , Kenichi Murano , Kazunori Ohno , Kenjiro Tadakuma , and Satoshi Tadokoro , *Fellow, IEEE*

Abstract—As considerable amounts of welding are required during ship construction, robotic automation is being promoted. However, current welding robots do not automate work in high or narrow places. One reason is that welding cannot be performed with sufficient accuracy because a welding robot with a torch cannot tow a heavy cable and thus may go off path. This letter proposes a multi-robot system for automating the execution of long welds in high and narrow places to address this problem. In the proposed method, towing vehicles are placed along the supply cable to reduce the load on the lead welding vehicle. In confined-space welding, the cable must not be excessively loaded, and obstacles such as walls must be avoided. Under the proposed method, autonomous movement of the towing vehicles is achieved by solving an optimization problem that considers these aims and minimizes the amount of change from the estimated current cable shape. The method was evaluated through simulation and real-world tests, in which it was applied successfully to tow the cable with a welding torch in a working area of $2.6 \times 10 \text{ m}^2$ (simulation) and of $3.4 \times 5.5 \text{ m}^2$ (real-world environment) without disturbing the lead vehicle's movement.

Index Terms—Autonomous vehicles, motion control, multi-robot systems.

I. INTRODUCTION

WELDING is one of the most critical manufacturing processes in the construction of large ships. Therefore, various robots have been introduced to save labor and reduce time. Many current welding robots are summarized in [1] and [2]. Most installed robots are large and are fixed on the ground, which prevents them from operating in high or narrow places. Mobile welding robots, on the other hand, have high portability; many of these have also been studied [2]–[11]. They include robots equipped with articulated manipulators [3], [4], [5] and robots that travel on walls via magnetic attraction [3]–[11].

Manuscript received 24 February 2022; accepted 26 April 2022. Date of publication 16 June 2022; date of current version 23 September 2022. This letter was recommended for publication by Associate Editor k. H. Petersen and Editor M. Ani Hsieh upon evaluation of the reviewers' comments. (*Corresponding author: Yoshito Okada.*)

Ryota Suzuki, Yoshito Okada, Yoshiki Yokota, Tatsuyoshi Saijo, Kazunori Ohno, Kenjiro Tadakuma, and Satoshi Tadokoro are with the Tohoku University, Sendai, Miyagi 980-8579, Japan (e-mail: suzuki.ryota@rm.is.tohoku.ac.jp; okada@rm.is.tohoku.ac.jp; yokota.yoshiki@rm.is.tohoku.ac.jp; saijo.tatsuyoshi@rm.is.tohoku.ac.jp; kazunori@rm.is.tohoku.ac.jp; tadakuma@rm.is.tohoku.ac.jp; tadokoro@rm.is.tohoku.ac.jp).

Haruhiko Eto, Yuya Sakai, and Kenichi Murano are with the Technology Research Center, Sumitomo Heavy Industries, Ltd., Shinagawa City, Tokyo 141-0032, Japan (e-mail: haruhiko.eto@shi-g.com; yuya.sakai.a@shi-g.com; kenichi.murano@shi-g.com).

Digital Object Identifier 10.1109/LRA.2022.3183529

These robots are designed for use in high or narrow places or for welding around uneven workpieces.

Even with the availability of mobile welding robots, however, it is not possible to perform long welds operations with a single such robot. One reason is the presence of a cable, which is required for supplying welding wire and gas to the welding torch. Even if the welding torch is carried by a small self-propelled mobile robot that can be used in high or narrow places, it cannot weld with sufficient accuracy because it cannot tow all of the heavy cable and thus can go off path. Although the traction force of the robot can be sufficiently strengthened, the robot becomes large and heavy as a result, rendering it unable to operate in narrow spaces. Instead, it is effective to automate long welds operations in narrow spaces by using a system consisting of several towing robots positioned along the cable and a lead welding robot to manipulate the cable.

However, most previous research on cable towing by multiple mobile robots has focused on the mechanism. For example, Ichimura et al. proposed a spherical tether-handling mechanism [12] that uses the same pair of actuators to feed the cable and drive the wheels. It is small and portable and can overcome steps up to 90.9% of the body's diameter. Hirose et al. developed Genbu (a snake-like robot) [13], which has multiple bodies connected by cable-shaped joints and can run at high speeds on uneven terrain owing to its passive-joint mechanism. In addition, limitation of the posture angle prevents the cable from breaking. However, the cable between vehicles cannot be very long because the mechanism transmits the force between vehicles by the elasticity of the joint.

Therefore, in this study, we focused on the planning and generation of motion for the towing of a welding cable by multiple mobile robots instead of on the mechanism. A plan for towing the cable is generated such that (i) the cable does not bend excessively, (ii) it does not come into contact with obstacles, and (iii) the change in cable shape is kept to a minimum so that the robots do not need to move rapidly. Then, the target positions of the towing robots are generated based on the desired cable shape, and the motion of the towing robots is executed. This letter proposes a method for guiding the towing robots by solving an optimization problem that addresses these requirements as an objective function together with the lead robot's position planned in advance as a constraint.

The remainder of this letter is organized as follows. In Section II, a multi-robot system that cooperatively tows a welding cable is proposed and compared conceptually with other systems. In Section III, the simulator used to develop and evaluate the multi-robot system is described; it consists of a multibody

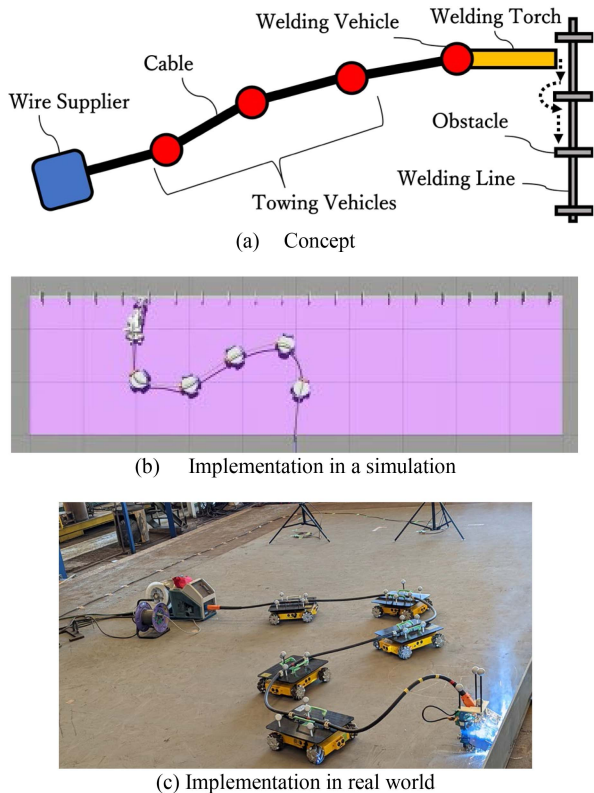


Fig. 1 Multi-robot system that tow a cable cooperatively; It implemented in a simulation and transferred into real world.

cable model and omnidirectional vehicles that simulate Omni Wheels with zero axial friction. In Section IV, the formulation of the optimization-based cable-towing method is introduced. In Section V, the proposed method is evaluated using results of simulations and welding tests in real-world environments. In Section VI, conclusions and prospects are presented.

II. OVERVIEW OF A MULTI-ROBOT SYSTEM FOR COOPERATIVE TOWING OF WELDING CABLES

Fig. 1(a) shows a conceptual diagram of a multi-robot system for cooperative towing of a welding cable. The proposed system consists of a welding vehicle and multiple cable-towing vehicles. The welding vehicle autonomously moves the welding torch along the welding line via locomotion and manipulators; the towing vehicles automatically follow the welding vehicle and cooperatively tow the cable. The welding torch and cables are distributed and transported by these vehicles to reduce the cable tension acting on the lead welding vehicle and maintain the positional accuracy of the welding work, thereby enabling automatic welding of lengths of 10 m or more in a narrow space, which has not been possible with conventional welding robots. Each vehicle is small enough to work in narrow spaces and powerful enough to carry a short segment of cable. Initially, this system will be applied to the butt welding of outer plates and suspended pieces, which are performed on a horizontal surface. In the future, the vehicles will be capable of magnetic attachment [2]–[11] to enable welding on curved surfaces and

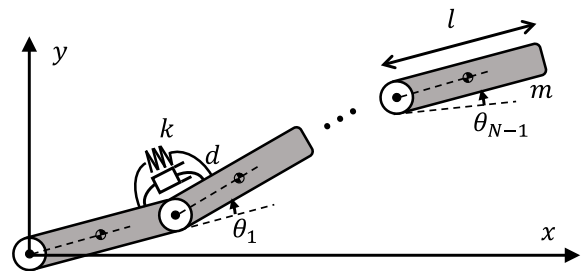


Fig. 2. Model of multi-link cable.

vertical surfaces. Manipulation of the welding torch by the welding vehicle is not described in this letter.

In work related to cable towing by multiple robots, Hirose et al. proposed the Whole Stem Drive [14], in which robots distribute the tension of cables and travel long distances for inspection within pipes. Because the piping has few obstacles, the proposal focuses on the mechanism and does not deal with motion planning. Our system, by contrast, plans the motion of the towing vehicles without interfering with the motion of the welding vehicle in a narrow space in which obstacles exist.

In addition, there have been related studies on optimizing cable placement via manipulation with articulated arms [15], [16], [17]. However, these did not consider bending radius as the target cable was relatively thin, and they simplified contact between the cable and the environment, representing it as a binary value (presence or absence).

Vehicles that manage cables by adjusting the cable length and tension using cable reels have been developed [18], [19]. In particular, [19] reports an example of cable untying while avoiding the obstacles in a multi-obstacle environment. However, because of the thinness of the target cable, the bending and twisting of the cable were not considered, as they are in the system we propose.

III. DEVELOPMENT OF WELDING CABLE TRACTION SIMULATOR

This section introduces the simulator built for the efficient development and evaluation of the cable-towing system proposed in Section II.

A. Cable

A simulation model of cable consisting of rigid links and joints was constructed to represent an actual welding cable (Fig. 2). Each of the N links is a rigid cylindrical body. Joints with three rotational degrees of freedom are placed between the links. Each degree of freedom has a rotational spring and a damper element.

The parameters of the model were identified by preliminary experiments using an actual cable and are listed in Table I. The weight of the cable was assigned to be the same as that of the actual cable. The friction μ of the cable surface was determined by measuring the friction angle. The coefficients of elasticity k (N·m/rad) and viscosity d (N·m·s/rad) in the direction of cable bending were adjusted to match the free end's balanced position and vibration behavior when the actual cable was cantilevered and fixed. The number of links, N , was set to 60 to balance the accuracy and speed of the simulation.

TABLE I
PARAMETERS OF CABLE MODEL

Parameter	Value	Parameter	Value
Link length l	0.10 m	Extinction coefficients d	0.15 N·m·s/rad
Cable radius r	8.5×10^{-3} m	Surface friction μ	0.87
Link mass m	0.10 kg	Number of links N	60
Elastic modulus k	1.7 N·m/rad		

TABLE II
PARAMETERS OF VEHICLE MODEL

Parameter	Value	Parameter	Value
Mass m	10.0 kg	Wheel width l_w	0.03 m
Body radius r_b	0.15 m	Wheel friction μ_1	0.50
Body height l_b	0.10 m	Axial friction μ_2	0.0
Wheel radius r_w	0.10 m		

B. Towing Vehicle

The vehicle used in this study need to be agile in a confined space for cable handling. Therefore, each vehicle is modeled as an omnidirectional vehicle equipped with four Omni Wheels. Instead of explicitly modeling the passive rollers, the Omni Wheels are simulated by cylindrical links with zero axial friction. This implementation was chosen to reduce the number of links and to improve the simulation speed.

The parameters of the model are shown in Table II. As the actual dimensions and weight of the vehicles were undecided at the time the simulator was built, the specifications of a typical small mobile robot were used as a reference.

C. Cable-Towing Simulation

The simulation of multiple robots towing a welding cable was constructed using the cable and vehicle models described in Sections. III-A and III-B. Fixed joints were established between the cable and each vehicle to simulate how the vehicle holds the cable. In the actual environment, the cable root is connected to the wire feeder, and therefore in the simulation world, fixed joints are likewise provided between the cable root and the origin. The total number of vehicles (welding vehicle plus towing vehicles) was six.

IV. CABLE TOWING USING OPTIMIZATION PROBLEM APPROACH

A. Cable Towing Based on Optimization

As mentioned in Section I, the cable-towing plan must satisfy three aims:

- 1) The cable should not be bent excessively for smoothly supplying welding wire and gas.
- 2) There should be no contact with obstacles.
- 3) Motion of the cable and robots should be minimized.

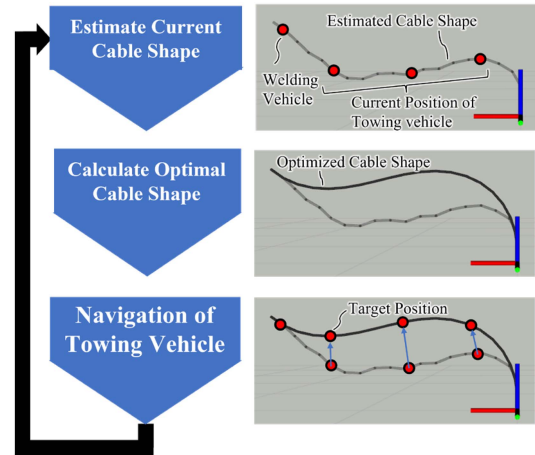


Fig. 3. Procedure for towing a cable based on optimization.

In addition, there is the constraint that one end of the cable is bound to the welding vehicle. The above aims are formulated as the objective function and constraint conditions of the optimization problem, and the cable shape to be achieved by traction is obtained.

Fig. 3 shows the procedure for the proposed optimization-based cable-towing method. The proposed method contains two optimization problems: one for estimating the current cable shape, and the other for calculating the optimal cable shape. In step 1, the first optimization problem with the current position of the welding and towing vehicles as a constraint is solved to estimate the current cable shape. Using the estimated solution as the initial value for the other optimization problem, the optimal shape adjacent to the current shape can be easily calculated. In step 2, using the estimated current cable shape as the initial value, the planned position of the welding vehicle as a constraint, and requirements (i) to (iii) above as the objective function, the second optimization problem is solved to obtain the optimal shape for the cable. In step 3, the target position is found on the optimal cable shape, and motion commands are sent to the towing vehicles that will cause the cable to assume the optimal shape. In present implementation, we use the optimal pose of cable link that the vehicle holds as the target pose of the vehicle. The vehicle tracks the target pose using a PID controller.

The advantage of this method is that it can be applied by simply attaching the vehicles to the welding cable in the field, as the shape of the cable is not explicitly measured but rather estimated from the vehicles' positions, which can be ascertained by the vehicles themselves.

The final goal of this research is to operate the multiple robots on a non-horizontal surface. In this study, however, the optimization problem was formulated with the assumption of a horizontal surface.

B. Cable Model to be Optimized

In the cable model to be optimized, the cable consists of rigid links connected by a bending joint with one degree of freedom, obtained by reducing the degrees of freedom of the simulation model shown in Fig. 2. As shown in Fig. 4, when the cable was



Fig. 4. Deflection of a cable between two vehicles.

attached to an actual vehicle, the vertical deflection was found to be slight, so it was decided to consider the cable in a two-dimensional plane, which is easier to handle mathematically. The reason for the low deflection is thought to be that the mount supports the cable near the vehicle and the elasticity of the cable is strong. The parameters to be optimized were a set of joint angles $\theta \in \mathbf{R}^N$.

C. Estimation of Current Cable Shape

This section describes the problem of estimating the current shape of a cable, which is solved in step 1 of the procedure described in Section IV-A.

1) *Formulation of the Optimization Problem:* The actual cable is considered to have a shape that minimizes the energy retained. For this study, we considered the energy retained by the cable as the sum of the strain energy proportional to the square of the joint angle and designed the objective function $f(\theta)$.

As the vehicles and the cable are geometrically constrained, an equality constraint $\mathbf{g}_{\text{vehicle}}(\theta)$ was established, to specify the point at which the cable passes through the current position of the vehicle. The optimization problem formulated based on the above is (1).

$$\begin{aligned} \text{Minimize } f(\theta) &= \sum_{i=0}^{N-1} \theta_i^2 \\ \text{Constraint : } g_{\text{vehicle}}(\mathbf{q}) &= 0 \end{aligned} \quad (1)$$

2) *Constraint to Fix Position and Orientation of Cable and Vehicle:* We designed the constraint $g_{\text{vehicle}} = [g_{x,m}(\theta)g_{y,m}(\theta)g_{\varphi,m}(\theta)]^t$, (2)(3)(4)

$$\begin{aligned} g_{x,m}(\theta) &= x_{m-1} + l\{\cos \varphi_{\text{start}} + \cos \varphi_{\text{start}+1} + \dots \\ &\quad + \cos \varphi_{\text{end}}\} - x_m \end{aligned} \quad (2)$$

$$\begin{aligned} g_{y,m}(\theta) &= y_{m-1} + l\{\sin \varphi_{\text{start}} + \sin \varphi_{\text{start}+1} + \dots \\ &\quad + \sin \varphi_{\text{end}}\} - y_m \end{aligned} \quad (3)$$

$$g_{\varphi,m}(\theta) = \varphi_{\text{end}} - \varphi_m, \quad (4)$$

in which $m \in \{1,2,3,4,5,6\}$, and $\varphi_i = \sum_{j=0}^i \theta_j$. φ_{start} is the attitude of the $(m-1)$ th vehicle, and φ_{end} is the attitude of the m th vehicle. l is the length of a cable link. This constraint ensures that the pose of the link in the cable fixed to the vehicle matches the pose of the vehicle.

D. Calculation of Optimal Cable Shape

This section describes the problem of calculating the optimal cable shape, which is solved in step 2 of the procedure described in Section IV-A.

1) *Formulation of the Optimization Problem:* The objective function must be designed to satisfy three minimization aims simultaneously:

- 1) The cable is not subjected to excessive bending stress. In other words, the bending angle of each joint in the cable is sufficiently slight.
- 2) The possibility of contact between the cable and obstacles is slight. In other words, the distance between the cable and obstacles is sufficiently large.
- 3) The optimal shape is easy to achieve. In other words, the current shape and the optimal shape are somewhat alike.

Therefore, we designed a function $f_{\theta}(\theta)$ to indicate the bending stress of the cable, a function $f_d(\theta)$ to indicate the possibility of contact with obstacles, and a function $f_c(\theta)$ to indicate the change from the current shape. After applying a loss function to each term, the objective function $f(\theta)$ was defined as a weighted sum of the three functions. The three minimization functions are described in Sections IV-D-2–IV-D-4, and the loss function is introduced in Section IV-D-5.

In addition, as the planned position of the welding vehicle leading the towing vehicles is defined in the welding plan, an equality constraint $\mathbf{g}_w(\theta)$ was established, which states that the welding vehicle and the tip of the restrained cable are in the same position. This constraint is described in Section IV-D-6.

The final optimization problem, addressing the above considerations, is (5).

$$\begin{aligned} \text{Minimize } f(\theta) &= w_q f_q(\theta) + w_d f_d(\theta) + w_c f_c(\theta) \\ \text{Constraint : } g_w(\theta) &= 0 \end{aligned} \quad (5)$$

2) *Objective Function i: Minimization of the Cable Stress:* The objective function $f_{\theta}(\theta)$, which represents the cable stress, should be designed to decrease its value as the joint angle between the links decreases. In this study, it was designed as (6).

$$f_{\theta}(\theta) = \sum_{i=0}^{N-1} \rho_{\theta} (\theta_i^2), \quad (6)$$

in which the loss function is applied to the square of the joint angle and then summed.

3) *Objective Function ii: Minimization of Obstacle Contact Possibility:* The objective function $f_d(\theta)$, which indicates the possibility of contact between the cable and the obstacles, was designed using the sum of the distances between each cable link and the nearest obstacle, as (7).

$$f_d(\theta) = \sum_{i=0}^{N-1} \rho_d \left(\sqrt{(p_{\text{obs},i} - p_{\text{cable},i}(\theta))^2} \right), \quad (7)$$

where $p_{\text{obs},i}$ is the location of the obstacle nearest to the i th link, and $p_{\text{cable},i}$ is the location of the i th link. The value of ρ_d is such that the greater the argument, the smaller the value of ρ_d . Therefore, the greater the distances between the cable and obstacles, the more f_d is reduced.

4) *Objective Function III: Minimization of the Difficulty to Realize the Optimal Cable Shape:* The objective function $f_c(\theta)$, which indicates the amount of change from the estimated value

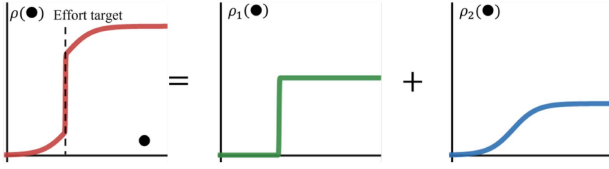


Fig. 5. Basic shape of the loss function.s.

of the current cable shape, was designed as (8).

$$f_c(\theta) = \sum_{i=1}^{N-1} \rho_c \left(\sqrt{(\theta_i - \theta_{i,\text{init}})^2} \right). \quad (8)$$

Its value increases as the difference between the estimated value of the current shape $\theta_{i,\text{init}}$ and the optimal solution θ_i of the cable shape optimization problem increases.

5) *Applying the Loss Function*: The functions $f_\theta(\theta)$, $f_d(\theta)$, and $f_c(\theta)$ described in Sections. IV-D-2–IV-D-4 are subjected to the loss function, given as (9).

$$\rho_\bullet(f) = \sum_{i=1}^2 a_i (\tanh(b_i(f - c_i)) + d_i). \quad (9)$$

The advantages of introducing this loss function are threefold. First, by making the range of values for $f_\theta(\theta)$, $f_d(\theta)$, and $f_c(\theta)$ finite, the weights in the objective function (5) can be easily adjusted. The loss function can have upper and lower asymptotes. In this study, we set the upper limit to 1 and the lower limit to 0 to facilitate the weight adjustment.

Fig. 5 shows the typical shape of the loss function, where the argument f is an arbitrary function.

The second advantage is that the loss function allows us to freely set the position of the inflection point and the slope of the curve surrounding it. In this study, we set the inflection point as the “effort target”, and the slope changes rapidly around this point. Thus, for example, if the bending angle of the cable exceeds a certain value, the value of the function will rapidly deteriorate, and the optimization algorithm will try to avoid exceeding that bending angle.

The third advantage is that the loss function is differentiable symbolically. The argument function in this study was also differentiable symbolically, and therefore symbolic differentiation, which is faster than automatic or numerical differentiation [20], [21], [22], can be used in the implementation.

6) *Constraint to Fix the Planned Position of the Welding Vehicle*: As previously mentioned, the position of the welding vehicle is planned before welding. Thus, it is necessary to set a constraint condition specifying that the planned position of the welding vehicle and the position of the cable tip bound to the welding vehicle must coincide. The formulation $\mathbf{g}_w = [g_x(\theta) \ g_y(\theta) \ g_\varphi(\theta)]^T$ was defined to match the cable tips with the planned positions x_w, y_w , and φ_w of the welding vehicle, as (10)(11)(12)

$$g_x(\theta) = x_0 + l\{\cos \varphi_0 + \dots + \cos \varphi_{N-1}\} - x_w \quad (10)$$

$$g_y(\theta) = y_0 + l\{\sin \varphi_0 + \dots + \sin \varphi_{N-1}\} - y_w \quad (11)$$

$$g_j(\theta) = \varphi_N - \varphi_w \quad (12)$$

in which $\varphi_i = \sum_{j=0}^i \theta_j$.

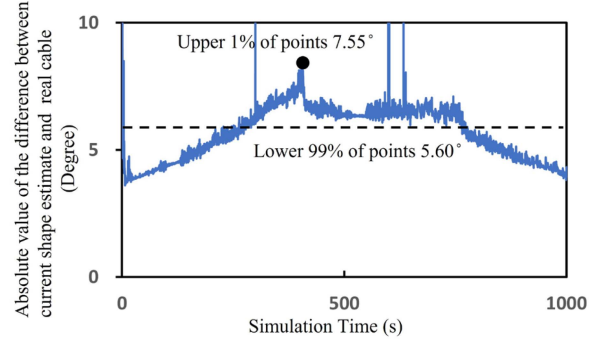


Fig. 6. Validity of the estimation of the current cable shape.

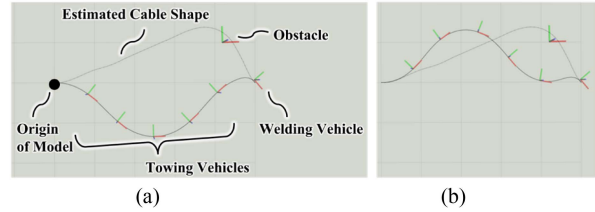


Fig. 7. Optimal cable shape based on optimization. (a) Without consideration of amount of change from current shape ($w_\theta = 24, w_d = 75, w_c = 0$); (b) with consideration of amount of change from current shape ($w_\theta = 24, w_d = 75, w_c = 1$).

V. EXPERIMENTS AND ANALYSIS

A. Validity of Estimation of Current Cable Shape

The method’s validity for estimating the current shape of a cable (described in Section IV-C) was evaluated. The evaluation was based on a simulation, which allowed us access to ground truth values such as the actual cable shape. The evaluation index was the absolute value of the difference between the estimated value and the actual value of the current cable shape when the cable is towed by towing vehicles navigated using the proposed method.

The starting position of the welding vehicle was (1.4 m, −4.8 m), and the target position was (1.4 m, 4.8 m). The coupled model of vehicles and cable described in Section III-C was used in the simulation. The total cable length was set to 6 m. The total number of vehicles (welding vehicle plus towing vehicles) was six. We used SLSQP [23] as an optimization algorithm, and NLOpt [24] as a library.

Fig. 6 shows the evaluation results, and the mean error for the lower 99% and upper 1% value of the errors. These results show that the formulation provides reasonable accuracy, as the average value per joint is within 6°.

B. Validity of Calculation of Optimal Cable Shape

The validity of the formulation of the optimization problem (described in Section IV-D) was evaluated by solving it with different conditions to obtain the optimal shape for the cable. The purpose of the evaluation was to confirm that the optimal shape can be adjusted by changing the weights in the objective function. In this evaluation, two types of solution were obtained: one without consideration of the amount of change from the

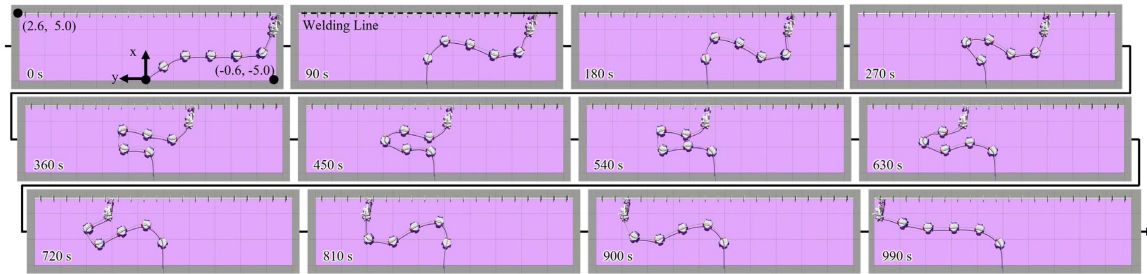


Fig. 8. Cable towing based on optimization (simulation).

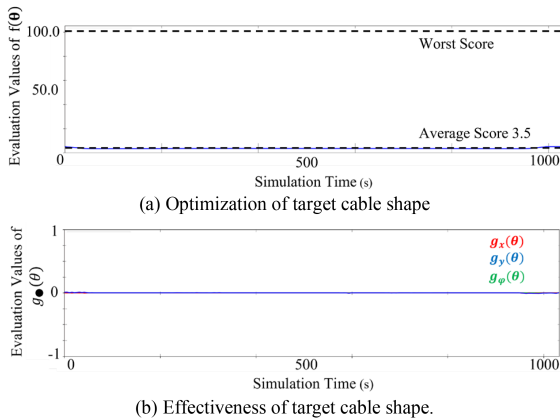


Fig. 9. Evaluation values for the problem of calculating the optimal shape for a cable (simulation).

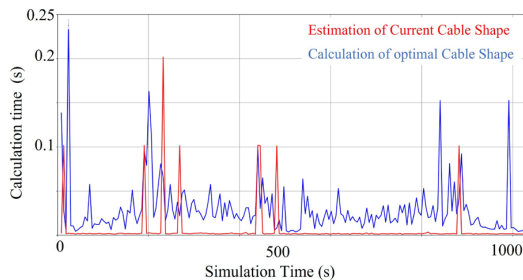


Fig. 10. Calculation Time of Optimization Problems.

TABLE III
MASS AND DIMENSIONS OF TOWING VEHICLE

Element	Value
Mass	4.2 kg
Chassis width	0.36 m
Chassis length	0.40 m
Chassis height	0.15 m

current shape ($w_\theta = 24$, $w_d = 75$, $w_c = 0$), and the other with ($w_\theta = 24$, $w_d = 75$, $w_c = 1$). The effort target of the objective function, $f_\theta(\theta)$, $f_d(\theta)$, and $f_c(\theta)$, were set to $(0.77 \text{ rad})^2$, 0.30 m , and 0.60 rad . The posture of the welding vehicle was set to $(5.0 \text{ m}, 0.0 \text{ m}, -\pi/4 \text{ rad})$, and an obstacle was positioned at $(4.2 \text{ m}, 1.0 \text{ m})$. The other conditions were the same as those described in Section V-A.

The results for the two solution types are shown in Fig. 7(a) and (b). In both, the shape of the cable with less bending stress is calculated by the effect of f_θ , and additionally, the distance between the cable and the obstacle was maintained by the effect of f_d . On the other hand, some differences were observed between the cable shapes in (a) and (b). In (a), as minimization of the change from the current shape was not considered, the solution was far from the current shape, which was not feasible to be realized in a short term. In contrast, the calculated solution shown in (b) is close to the current shape. These results confirm that the objective function and constraint conditions are reflected in the solution as intended.

C. Welding Simulation

The entire procedure for the proposed method was evaluated based on a simulation in which the cable was towed by vehicles navigated using the proposed method. The evaluation indices were 1) whether the behavior of the towing vehicles does not interfere with the movement of the welding vehicle, 2) the evaluation values for the optimal cable shape as given by the objective function and the constraint function, and 3) calculation time for solving the optimization problems.

The root of the cable was constrained to $(0.0 \text{ m}, 0.0 \text{ m})$. The traversable area was a rectangle with vertices at $(2.6 \text{ m}, 5.0 \text{ m})$ and $(0.0 \text{ m}, -5.0 \text{ m})$. The four sides of the area were defined as obstacles so that deviating outside the traversable area could be avoided. The welding vehicle was moved in a straight line from $(2.6 \text{ m}, -4.8 \text{ m})$ to $(2.6 \text{ m}, 4.8 \text{ m})$, for assumed welding along the upper edge of the area. The speed of motion was set to 600 mm/min , referring to the speed for general welding. The weights in the objective function were set as $w_\theta = 75$, $w_d = 24$, and $w_c = 1$. The other conditions were the same as those described in Section V-A.

Fig. 8 shows snapshots from the simulation. It was confirmed that the towing vehicles could be guided without interfering with the operation of the welding vehicle. Fig. 9(a) and (b) show the time-series data of the evaluation values for the problem of calculating the optimal shape for the cable. It is confirmed from Fig. 9(a) that the evaluation values as calculated by the objective function averaged 3.5 for the worst-case value of 100. The small increases in evaluation values at the start and end of welding are not relevant, as these occur simply because the cable bound to the welding vehicle approaches the boundary of the work area according to the welding plan. It was confirmed that behavior of the towing vehicles that did not interfere with the movement of the welding vehicle could be generated by successful solution of the optimization problem we developed.

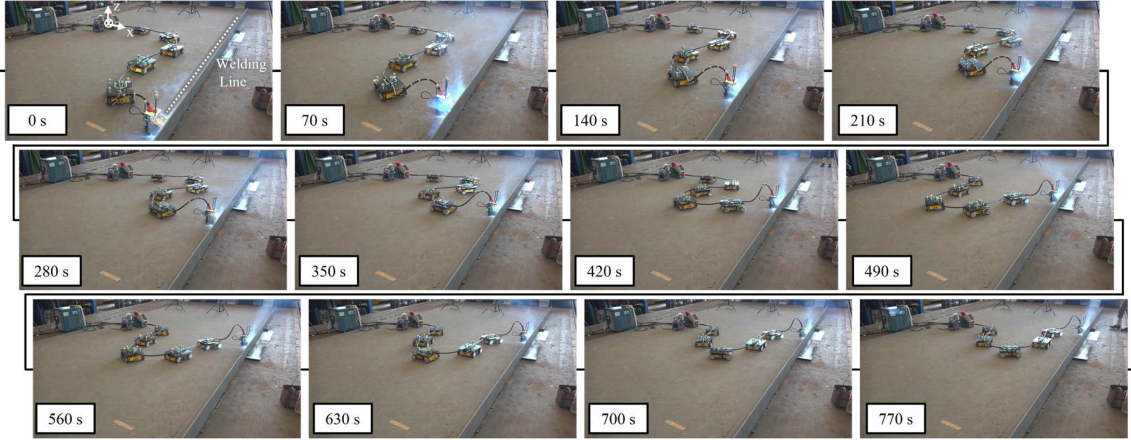


Fig. 11. Cable towing based on optimization (real world).

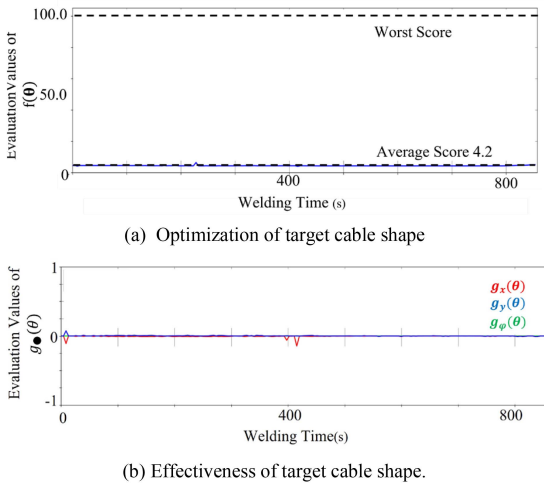


Fig. 12. Evaluation values for the problem of calculating the optimal shape for a cable (real world).

In addition, Fig. 9(b) shows that the evaluation value given by the constraint function is nearly zero. This result shows that the optimal solution satisfying the constraint conditions is calculated.

Fig. 10 shows the calculation time during the simulation. Fig. 10 shows the average calculation time of 22 Hz. This calculation time is much faster than 10 Hz, which is the operation period of the actual system test introduced in the next section. In other words, it shows that the proposed system can be executed in real-time. The short solution time is thought to be that all objective and constraint functions are implemented using symbolic differentiation, which can be computed quickly.

D. Welding in Real-World Experiment

The proposed method was further evaluated on an actual welding site. The evaluation indices were 1) the appearance of the motion of vehicles and cable, 2) the evaluation value for the optimal shape as given by the objective function and the constraint function, and 3) the movement trajectory of the

welding vehicle when the towing vehicles tow the welding cable in the motion planned by the proposed method.

The root of the cable was defined as the reference coordinate (0.0 m, 0.0 m). The towing vehicle was a Vstone Mecanum-wheeled robot [25] with a 0.05-m-high cable mount fixed to it. Table III shows the mass and dimensions of the towing vehicle. The position of each vehicle was obtained using motion capture (OptiTrack). A rectangle with vertices at (−0.20 m, −4.2 m) and (3.2 m, 1.4 m) was used as the traversable area, which was the same as the measurable area of the motion capture and is comparable to a typical actual welding area in the construction of large ships. Welding was performed along the upper edge of the area. The welding vehicle was moved in a straight line from (2.8 m, −4.2 m) to (2.8 m, 1.4 m). The travel speed was set to 330 mm/min, which is the usual speed in actual welding operations. The welding vehicle used was the robot described in [4]. The weights in the objective function were set as $w_\theta = 75$, $w_d = 20$, and $w_c = 5$. The other conditions were the same as those described in Section V-A.

The results of the welding tests are shown in Fig. 11. As in the previous evaluation via the simulation, it was confirmed that the towing vehicles could be guided without interfering with the motion of the welding vehicle. Contact between the welding vehicle and the towing vehicles did not occur.

Fig. 12(a) and (b) show the time-series data of the evaluation values for the problem of calculating the optimum cable shape. The calculated solution had an average evaluation value of 4.2 for the objective function. The evaluation value for the constraint function remained nearly zero, confirming the validity of the formulation.

In addition, the linearity of the moving path of the welding vehicle was evaluated using the coefficient of determination R^2 . The value of R^2 was 0.997, and it was confirmed that the welding vehicle moved without deviating from the target path.

E. Avoidance of Moving Obstacle in Real-World Environment

We tested whether the proposed system could autonomously maintain the optimal cable shape in a scenario in which an alien vehicle towing another cable approaches the towing vehicles.

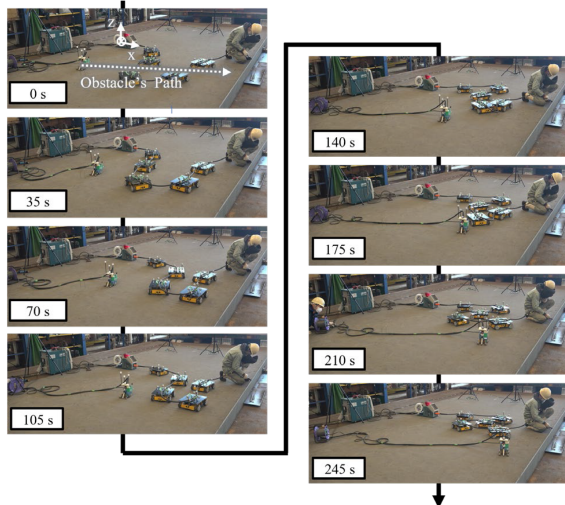


Fig. 13. Avoidance of moving obstacle (real world).

In this test, a situation in which a welder is welding at a fixed point was assumed. The position of the welder was set as (2.8 m, 1.0 m), and the alien vehicle was moved in a straight line from (0.34 m, -2.9 m) to (3.4 m, -2.8 m) at a speed of 600 mm/min. The other conditions were the same as those corresponding to the simulation described in Section V-C. Fig. 13 shows the test results. It was confirmed that a towing vehicles can be guided to avoid contact with the alien vehicle without overloading the cable.

VI. CONCLUSION

This letter presents the concept of a multi-robot system for cooperatively towing a welding cable, including estimation of the current cable shape and planning of the optimal cable shape, both based on optimization. The latter optimization problem was formulated to minimize the stress on the cable, the possibility of contact with obstacles, and the amount of change between the estimated value of the current shape and the optimal shape. The proposed method was evaluated via simulation and in actual environments, which demonstrated that it was possible to tow a welding cable in a traversable area of $2.6 \times 10 \text{ m}^2$ in the simulation and of $3.4 \times 5.5 \text{ m}^2$ in a real-world environment without hindering the lead welding vehicle's travel. In the future, we will extend the current optimization problem to three dimensions to plan operations on assumed steps and slopes occurring in an actual environment and enable handy pose estimation of vehicles [26]. These are steps toward the ultimate aim of expanding the use of automated welding in shipbuilding operations to save labor and time by improving the capabilities of mobile welding robots to work effectively in high or narrow spaces.

REFERENCES

- [1] D. Lee, "Robots in the shipbuilding industry," *Robot. Comput.-Integr. Manuf.*, vol. 30, no. 5, pp. 442–450, Oct. 2014.
- [2] A. G. Dharmawan, A. A. Vibhute, S. Foong, G. S. Soh, and K. Otto, "A survey of platform designs for portable robotic welding in large scale structures," in *Proc. 13th Int. Conf. Control Automat. Robot. Vis.*, 2014, pp. 1683–1688.
- [3] M. Wu, G. Pan, T. Zhang, S. Chen, F. Zhuang, and Z. Yan-zheng, "Design and optimal research of a non-contact adjustable magnetic adhesion mechanism for a wall-climbing welding robot," *Int. J. Adv. Robot. Syst.*, vol. 10, no. 1, Jan. 2013, Art. no. 63.
- [4] H. Eto and H. H. Asada, "Development of a wheeled wall-climbing robot with a shape-adaptive magnetic adhesion mechanism," in *Proc. IEEE Int. Conf. Robot. Automat.*, 2020, pp. 9329–9335.
- [5] L. Han, L. Wang, J. Zhou, and Y. Wang, "The development status of ship wall-climbing robot," in *Proc. 4th Int. Conf. Electron Device Mech. Eng.*, 2021, pp. 231–237.
- [6] T. P. Sattar, M. Alaoui, S. Chen, and B. Bridge, "A magnetically adhering wall climbing robot to perform continuous welding of long seams and non-destructively test the welds on the hull of a container ship," Accessed: Feb. 22, 2022. [Online]. Available: <http://www.wseas.us/e-library/transactions/mechanics/2008/32-238.pdf>
- [7] F. Yanqiong and S. Libo, "Design and analysis of modular mobile robot with magnetic wheels," *WSEAS Trans. Appl. Theor. Mechanics*, vol. 3, no. 12, pp. 901–911, 2008.
- [8] J. Li and X.S. Wang, "Novel omnidirectional climbing robot with adjustable magnetic adsorption mechanism," in *Proc. 23rd Int. Conf. Mechatronics Mach. Vis. Pract.*, 2016, pp. 1–5.
- [9] O. Kermorgant, "A magnetic climbing robot to perform autonomous welding in the shipbuilding industry," *Robot. Comput.-Integr. Manuf.*, vol. 53, pp. 178–186, 2018.
- [10] J. Hu, X. Han, Y. Tao, and S. Feng, "A magnetic crawler wall-climbing robot with capacity of high payload on the convex surface," *Robot. Auton. Syst.*, vol. 148, pp. 1–12, 2022.
- [11] Z. Mao, J. Pan, and H. Zhang, "Mobile welding robot system based on rotating arc sensor applied for large fillet welding seam tracking," in *Proc. 6th Int. Conf. Natural Comput.*, 2010, pp. 394–397.
- [12] T. Ichimura, K. Tadakuma, E. Takane, M. Konyo, and S. Tadokoro, "Development of a spherical tether-handling device with a coupled differential mechanism for tethered teleoperated robots," in *Proc. IEEE/RSJ Int. Conf. Intell. Robots Syst.*, 2016, pp. 2604–2609.
- [13] H. Kimura and S. Hirose, "Development of Genbu: Active wheel passive joint articulated mobile robot," in *Proc. IEEE/RSJ Int. Conf. Intell. Robots Syst.*, 2002, pp. 823–828.
- [14] S. Hirose, H. Ohno, T. Mitsui, and K. Suyama, "Design of in-pipe inspection vehicles for $\phi 25$, $\phi 50$, $\phi 150$ pipes," in *Proc. IEEE Int. Conf. Robot. Automat.*, 1999, pp. 2309–2314.
- [15] J. Zhu, B. Navarro, P. Fraisse, A. Crosnier, and A. Cherubini, "Dual-arm robotic manipulation of flexible cables," in *Proc. IEEE/RSJ Int. Conf. Intell. Robots Syst.*, 2018, pp. 479–484.
- [16] D. Sánchez, W. Wan, and K. Harada, "Tethered tool manipulation planning with cable maneuvering," *IEEE Robot. Automat. Lett.*, vol. 5, no. 2, pp. 2777–2784, Apr. 2020.
- [17] A. Sintov, S. Macenski, A. Borum, and T. Bret, "Motion planning for dual-arm manipulation of elastic rods," *IEEE Robot. Automat. Lett.*, vol. 5, no. 4, pp. 6065–6072, Oct. 2020.
- [18] J. E. Naglak *et al.*, "Cable deployment system for unmanned ground vehicle (UGV) mobile microgrids," *HardwareX*, vol. 10, Oct. 2021, Art. no. e00205.
- [19] V. A. K. T. Rajan, A. Nagendran, A. Dehghani-Sanij, and R. C. Richardson, "Tether monitoring for entanglement detection, disentanglement and localisation of autonomous robots," *Robotica*, vol. 34, no. 3, pp. 527–548, Mar. 2016.
- [20] A. Griewank, "On automatic differentiation," Accessed: Feb. 24, 2022. [Online]. Available: <https://citeseerx.ist.psu.edu/viewdoc/download?doi=10.1.1.54.2317&rep=rep1&type=pdf>
- [21] C. J. F. Ridders, "Accurate computation of $F'(x)$ and $F''(x)$ $F'(x)$," *Adv. Eng. Softw.*, vol. 4, no. 2, pp. 75–76, 1978.
- [22] Google, Ceres Solver – Automatic Derivatives, Accessed: May 10, 2022. [Online]. Available: http://ceres-solver.org/automatic_derivatives.html
- [23] D. Kraft, "A software package for sequential quadratic programming," Institut für Dynamik der Flugsysteme, Oberpfaffenhofen, Germany, Tech. Rep. DFVLR-FB 88-28, Jul. 1988.
- [24] S. G. Johnson, "NLOpt (library for nonlinear optimization)," Accessed: Feb. 18, 2022. [Online]. Available: <http://github.com/stevengj/nlopt>
- [25] Vstone Co., Ltd., "4WD 100mm mecanum wheel robot," Vstone, Accessed: Feb. 18, 2022. [Online]. Available: https://www.vstone.co.jp/robotshop/index.php?main_page=product_info&cPath=156_311_312&products_id=5138/
- [26] Y. Okada, D. Fujikura, Y. Ozawa, K. Tadakuma, K. Ohno, and S. Tadokoro, "HueCode: A Meta-marker exposing relative pose and additional information in different colored layers," in *Proc. IEEE Int. Conf. Robot. Automat.*, 2021, pp. 5928–5934.